

# Reduction of nitrogen oxide in N<sub>2</sub> by NH<sub>3</sub> using intermittent dielectric barrier discharge

Mitsunori Nishida and Ken Yukimura<sup>a)</sup>

*Department of Electrical Engineering, Faculty of Engineering, Doshisha University, Kyotanabe, Kyoto 610-0321, Japan*

Shinji Kambara

*Idemitsu Kosan Company, Sodegaura, Chiba 299-0267, Japan*

Toshiro Maruyama<sup>b)</sup>

*Department of Chemical Engineering, Graduate School of Engineering, Kyoto University, Kyoto 606-8501, Japan*

(Received 8 March 2001; accepted for publication 22 June 2001)

NO in N<sub>2</sub> gas was removed by injecting ammonia radicals, which were externally generated by flowing the NH<sub>3</sub> gas diluted with Ar gas through dielectric barrier discharge with a one-cycle sinusoidal-wave power source. The NO reduction for changes in both the applied voltage and the repetition rate was well correlated with the discharge power, which was proportional to the total discharge time per unit time. There was an optimum NH<sub>3</sub> concentration in the narrow concentration window for the energy efficiency of NO reduction at a fixed discharge power. The maximum energy efficiency was obtained at small values of the NH<sub>3</sub> concentration and the discharge power. The low NH<sub>3</sub> concentration effectively increased the energy efficiency by drastically decreasing the discharge-firing voltage. © 2001 American Institute of Physics. [DOI: 10.1063/1.1394902]

## I. INTRODUCTION

The thermal reduction and elimination of the nitrogen oxide (NO<sub>x</sub>) from postcombustion gases via ammonia (NH<sub>3</sub>) addition<sup>1</sup> have been used in burning technology. Modeling results of the thermal de-NO<sub>x</sub> process are particularly sensitive to the branching ratio:



Equation (1) gives a termination reaction, while Eq. (2) indicates a source of OH as well as H (from NHN dissociation). These radicals are key to sustaining the chain reaction.<sup>2,3</sup> Recently, nonthermal plasma processes<sup>4–13</sup> were proposed to use for the NO<sub>x</sub> removals at lower temperatures. The plasma processes have attracted attention because of their low instrumental costs and simple process, where the plasma-induced radicals efficiently convert NO<sub>x</sub> into harmless gases such as N<sub>2</sub>, O<sub>2</sub>, and H<sub>2</sub>O. Nonthermal plasmas can be produced either by electron-beam irradiation<sup>12,13</sup> or by electrical discharge method.<sup>4–11,13</sup> Concerning electrical discharge methods, the dielectric barrier discharge (silent discharge),<sup>8,11</sup> the corona discharge,<sup>4–7,11</sup> and the surface discharge have been reported. This study used the dielectric barrier discharge at atmospheric pressure. The dielectric barrier discharge is driven by self-extinguishing very short pulses of high voltage, thus creating short-lived discharge plasmas that consist of energetic electrons, which efficiently produce the radicals for the NO<sub>x</sub> removal. Additional advan-

tages of the dielectric barrier discharge are that a low-cost treatment is possible without using the vacuum system, and that the durable years of the apparatus are prolonged, because the materials which are inert to NO<sub>x</sub>, ammonia, and its radicals can be used as dielectric materials.

In the usual electrical discharge methods, the plasma is produced in the discharge volume, where the reaction gas such as ammonia is mixed with NO<sub>x</sub>. This study used the method of radical injection,<sup>5–7,9–11</sup> where the ammonia radicals were externally generated in a separate chamber of a small volume through electron-impact dissociation and ionization, and were injected in NO<sub>x</sub> gas to reduce/or oxidize the NO<sub>x</sub> molecules. Therefore, the method of radical injection is efficient in large-scale NO<sub>x</sub> removal.

This study concerns the removal via reduction process,<sup>9–11</sup> while the reported studies have mainly concerned about the NO<sub>x</sub> removal via oxidation process.<sup>4–8</sup> Kinetic modeling by Zhou *et al.*<sup>9,10</sup> indicated that the NH<sub>2</sub> radicals, which are externally generated and injected into flue gas, were capable of reducing a large amount of NO<sub>x</sub> at temperatures well below the limit of the thermal de-NO<sub>x</sub> process. In their experiments NO<sub>x</sub> was reduced by injecting ammonia radicals, which were externally generated by flowing the NH<sub>3</sub> gas diluted with Ar gas through inductively coupled plasma system. Penetrante *et al.*<sup>11</sup> compared the electrical energy consumption of different kinds of nonthermal plasma reactors with regards to the electron-impact dissociation of N<sub>2</sub> and the subsequent reduction of NO by the nitrogen atom. They showed that the energy cost for reduction of NO, 240 eV, was simply the energy cost for production of N radical.

In this study, NO in N<sub>2</sub> gas was reduced by the ammonia

<sup>a)</sup>Electronic mail: kyukimur@mail.doshisha.ac.jp

<sup>b)</sup>Electronic mail: maruyama@cheme.kyoto-u.ac.jp

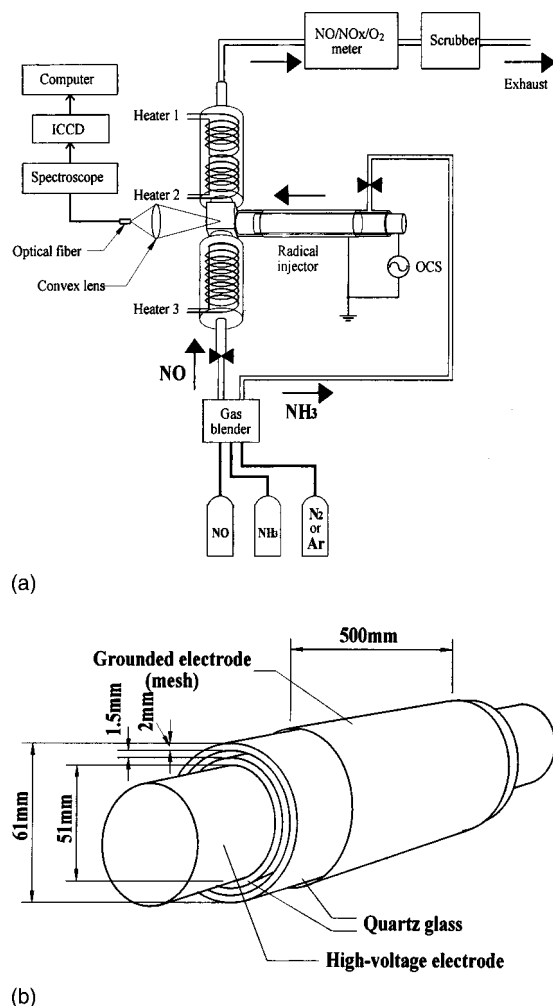


FIG. 1. Schematic diagrams of (a) experimental apparatus and (b) radical injector with its dimensions.

radicals, which were generated by flowing the NH<sub>3</sub> gas diluted with Ar gas through dielectric barrier discharge with a one-cycle sinusoidal (OCS)-wave power source. Ar gas was used to minimize generation negative ions near the discharge zone and to maximize electron impact ammonia dissociations.<sup>7</sup> The ammonia radicals were injected to a reaction chamber, and were mixed with the NO gas diluted with N<sub>2</sub>. Among the ammonia radicals, NH<sub>2</sub>, NH, and N, the NH<sub>2</sub> radical is considered the primary reducing agent. The NO reduction and its energy efficiency are discussed based on the experimental results for wide ranges of the ammonia concentration and the discharge power of the plasma.

## II. EXPERIMENT

Figure 1 shows schematic diagrams of the nitric oxide (NO) reduction system and the radical injector. The system consists of two chambers: one used as an unheated radical injector for producing ammonia radicals, and the other as a heated reaction chamber for decomposing the NO gas by mixing it with the ammonia radicals generated in the radical injector. In this system, the ammonia radicals were produced from ammonia gas without directly exposing the NO gas to

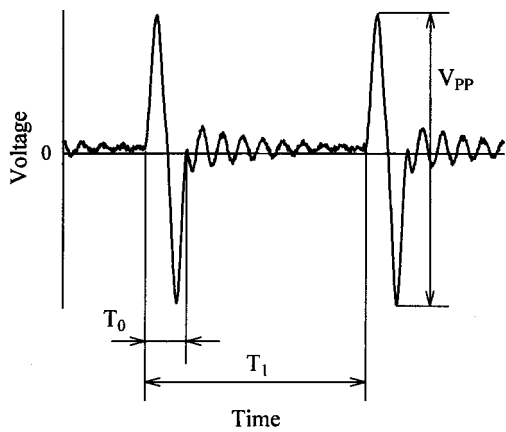
the plasma. The NO removal reaction was initiated by injecting the ammonia radical into the reaction chamber.

The electrodes are coaxial in configuration with quartz glass tubes as dielectric materials. The outer glass tube is 61 mm in diameter and 2 mm thick, while the inner glass tube is 50 mm in diameter and 2 mm thick. Thus, the gap between the outer and inner glass tube is 1.5 mm. The dielectric barrier discharge occurred at the gap. The metallic electrodes covered both the outer side of the outer glass tube and the inner side of the inner glass tube. The grounded outer electrode is made of a mesh steel sheet, and the inner electrode is made of stainless steel. The inner electrode can be cooled by tap water during the application of the high voltage. In this study, however, the cooling of the electrode was not needed because of the use of the intermittent power source.

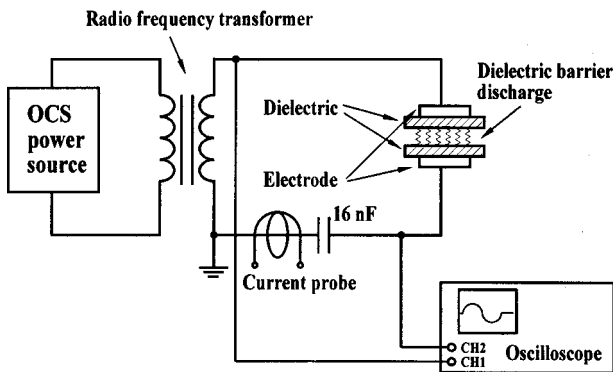
NO gas was diluted with nitrogen, and ammonia was diluted with argon gas. The concentration and flow rate of NO and NH<sub>3</sub> were adjusted in the gas blender by mixing with nitrogen and argon gas. The NO concentration was 1000 ppm by volume, and the gas flow rates were 1.5, 2, and 4 l/min. The NH<sub>3</sub> concentration was in a range of 0.1%–3% by volume, and the gas flow rates was 0.5 l/min. The adjusted NO gas was fed in the reaction chamber of 50 mm in diameter and 1.3 m long, and the adjusted NH<sub>3</sub> gas was fed to the radical injector. The concentrations of NO, NO<sub>2</sub>, and O<sub>2</sub> were measured before and after plasma processing. The concentration of the de-NO<sub>x</sub> gas after flowing through the reaction chamber was measured with a NO<sub>x</sub> meter (Shimadzu NOA-7000) set at the exit. The data were single point measurements. The NO reduction is defined as the ratio of NO reduced to the initial concentration of NO.<sup>9</sup> During the experiment, the reaction temperature was kept constant in the range of 350–600 °C. The temperature was measured at the mixing area.

The dielectric barrier discharge was produced with an intermittent power source. Figure 2(a) schematically shows the waveform of the applied one-cycle sinusoidal voltage. The repetition rate  $R_R$  is defined as the reciprocal of the repetition time  $T_1$  of the discharge.  $T_0$  was approximately 10  $\mu$ s, and  $R_R$  was 5–50 kHz. That is, the one-cycle sinusoidal voltage was intermittently applied to the gap for a duration of 10  $\mu$ s at a repetition rate of 5–50 kHz.

Figure 2(b) shows a schematic diagram of the electric circuit for producing a dielectric barrier discharge and for measuring electric characteristics. The output peak-to-peak voltage of the power supply was 5–20 kV. The voltage was raised by a pulse transformer (winding ratio of 1:15). The accumulated charge was obtained from the voltage across a series capacitor (16 nF) that was connected on the side of the ground in a circuit. The energy input during one cycle of the dielectric barrier discharge was estimated from the accumulated charge and voltage across the output windings of the transformer using the  $V$ - $Q$  curve of the Lissajous figure. The time evolutions of source voltage, current, and accumulated charge were simultaneously monitored with an oscilloscope.



(a)



(b)

FIG. 2. One-cycle sinusoidal power source. (a) Waveform of voltage supplied from a one-cycle sinusoidal power source, and (b) circuit for measurements of electric characteristics.

### III. RESULTS AND DISCUSSION

A visual observation of the plasma in the radical injector showed no feature of the filamentary discharge, and the current waveform observed with the oscilloscope showed no series of spikes, which is characteristic of the filamentary discharge. These facts strongly suggest that the plasma is a diffused glow-like discharge. Figure 3 shows the  $V-Q$  curve of the Lissajous figure for the discharge at an applied voltage of 10 kV and at a  $\text{NH}_3$  concentration of 1%. The slope of the curve represents the composite capacitance of both the di-

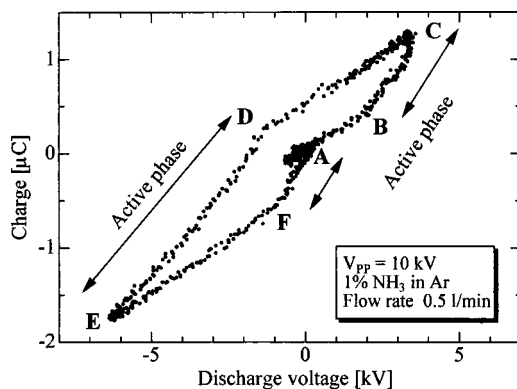


FIG. 3.  $V-Q$  Lissajous figure.

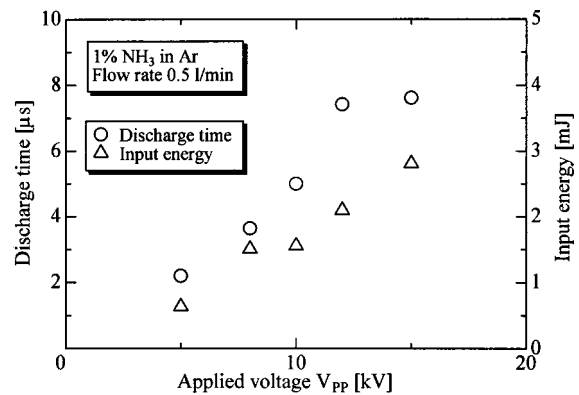
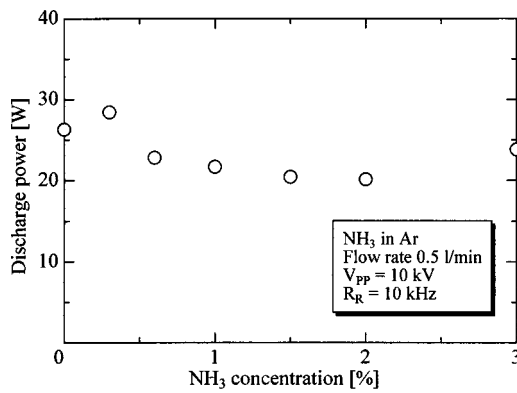


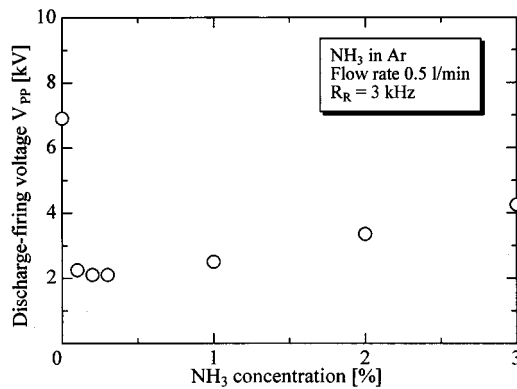
FIG. 4. Discharge time and input energy as a function of applied voltage.

electric material and the gap. Thus it becomes small when discharge occurs. During the cycle starting from A, the discharge occurs only during B-C, D-E, and F-A in one cycle. The figure is not like a parallelogram, which is a typical form for dielectric barrier discharge. This is because the voltage wave is not ac but intermittent one cycle sinusoidal of a period of 10  $\mu\text{s}$ . Figure 4 shows the total discharge time and the energy input per one cycle of sinusoidal as a function of the applied voltage. The total discharge time increases with increasing applied voltage, and hits the ceiling of about 8  $\mu\text{s}$  at above 12 kV. The energy input per one cycle increases with increasing the applied voltage. Thus, the increase in energy input is attributable to the increase of total discharge time at an applied voltage below 12 kV due to a fixed value of energy input per one pulse of discharge, because the voltage applicable to the gap during discharge is fixed by the dielectric electrodes. When the applied voltage was further increased from 18 kV, the shining lines were frequently observed to occur in plasma, and the discharge became unstable. Thus, under the experimental conditions of this study (the applied voltage is below 18 kV) the excitation intensity of plasma is not changed, and the energy input per one cycle is increased by increasing the total discharge time.

Figure 5(a) shows the discharge power at 10 kV as a function of  $\text{NH}_3$  concentration. The discharge power is approximately constant, i.e., about 23 kW, showing a weak dependence on  $\text{NH}_3$  concentration. Figure 5(b) shows the discharge-firing voltage as a function of  $\text{NH}_3$  concentration. The measured discharge-sustain voltage was a little less than the discharge-firing voltage. For pure Ar gas, the discharge-firing voltage is 6.8 V. When a small quantity of  $\text{NH}_3$  is mixed with Ar gas, the discharge-firing voltage drastically decreases to 2 kV at  $\text{NH}_3$  concentrations of 0.1%–0.3%, and then slowly increases with increasing  $\text{NH}_3$  concentration. Thus, the low concentration of  $\text{NH}_3$  is effective to decrease the discharge power of radical injector. This fact is attributable to the Penning ionization. That is, the excited Ar atoms in metastable state ( $4^3P_2$  and  $4^3P_0$ ) ionize  $\text{NH}_3$  molecules, because the excitation energies (11.55 and 11.72 eV) of  $\text{Ar}(4^3P_2)$  and  $\text{Ar}(4^3P_0)$  are larger than the ionization energy (10.85 eV) of  $\text{NH}_3$ . It is expected that the dischargeable voltage can be further lowered by the additional mixing of a small quantity of other gas.



(a)



(b)

FIG. 5. Discharge characteristics: (a) discharge power as a function of NH<sub>3</sub> concentration, and (b) discharge-firing voltage as a function of NH<sub>3</sub> concentration.

Figure 6 shows the NO reduction as a function of reaction temperature. NO is not reduced at a temperature below 500 °C. It is partly reduced at a temperature above 500 °C, and is completely reduced at about 600 °C. When the discharge was switched off, NO was not reduced at these temperatures. It is noted that the electron impacts efficiently dissociate NH<sub>3</sub> at a low temperature, although NH<sub>3</sub> is not thermally dissociated at a temperature below 900 °C. The measured low temperature indicates that the NO reduction reaction of this study is triggered only by plasma effect. The following results were obtained at a reaction temperature of 600 °C.

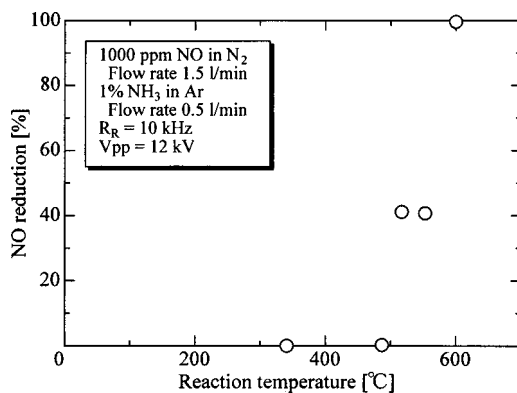


FIG. 6. NO reduction as a function of reaction temperature.

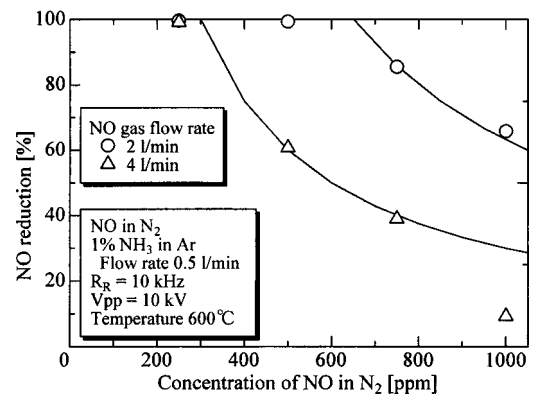
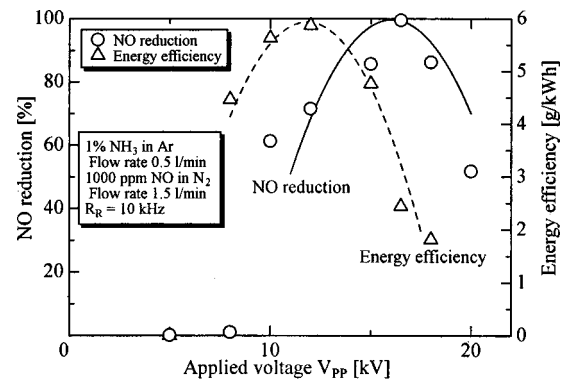
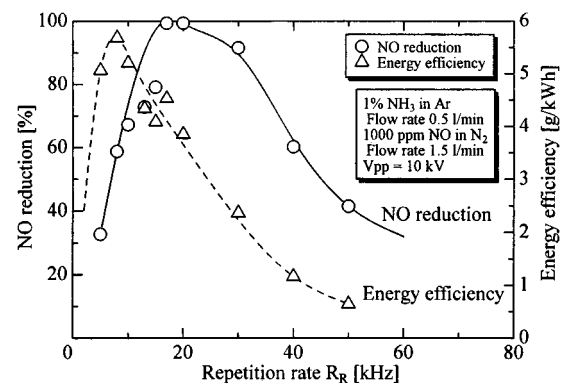


FIG. 7. NO reduction as a function of NO concentration.

Figure 7 shows the NO reduction for two kinds of NO gas flow rates as a function of the NO concentration. The NO reduction decreases with increasing NO concentration, the reduction for 4 l/min being lower than that for 2 l/min. All the data, except for that at 1000 ppm for 4 l/min, are well correlated with the solid lines, which show a constant volumetric NO reduction rate of 1.2 cm<sup>3</sup>/min. That is, the molar NO reduction rate is constant, i.e.,  $5.36 \times 10^{-5}$  mol/min, for the NH<sub>3</sub> flow rate of  $22.3 \times 10^{-5}$  mol/min and is independent of the flow rate and the concentration of NO gas. Thus the NO reduction is not limited by the chemistry of the process, but rather by the ability to generate ammonia radicals effectively and to provide favorable conditions for the introduc-

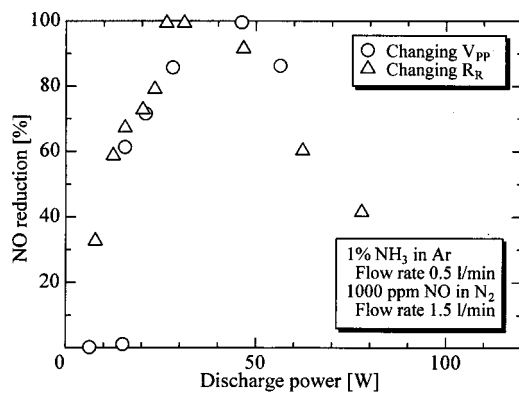


(a)

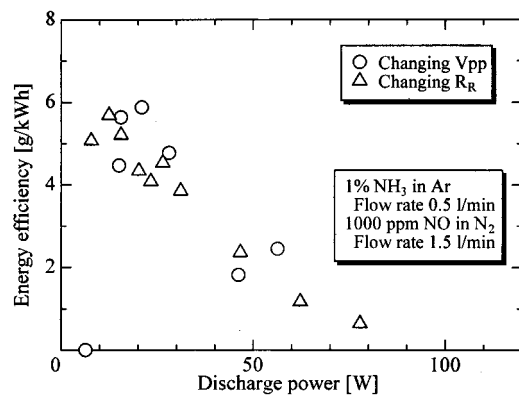


(b)

FIG. 8. NO reduction and its energy efficiency as functions of (a) applied voltage  $V_{pp}$  and (b) repetition rate.



(a)



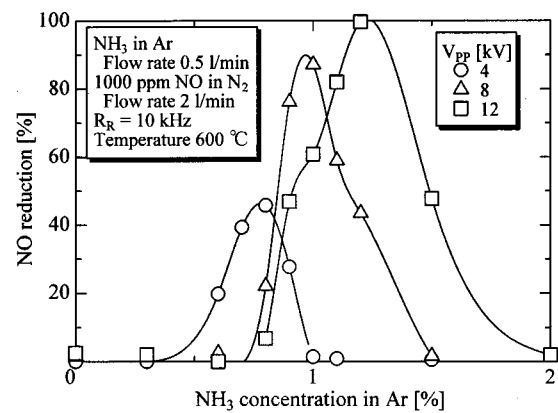
(b)

FIG. 9. Discharge power dependencies of (a) NO reduction and (b) energy efficiency.

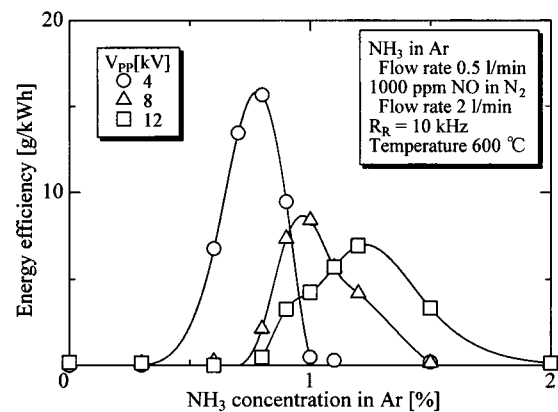
tion to NO gas flow and mixing with it. The following discussions are based on the results, obtained at the NO concentration of 1000 ppm and at gas flow rates of 1.5 and 2 l/min.

Figure 8 shows the NO reduction and its energy efficiency at a  $\text{NH}_3$  concentration of 1% as a function of applied voltage  $V_{pp}$  and repetition rate  $R_R$ , respectively. The energy efficiency is defined as the mass flow rate of reduced NO per input electrical power. The results obtained by changing both the applied voltage and repetition rate show the same trend, showing optimum conditions of the discharge for the decomposition of  $\text{NH}_3$  into the radicals, which reduce NO efficiently. That is, the NO reduction shows the maximum values at a repetition rate of 20 kHz and at an applied voltage of 16 kV, while the energy efficiency shows the maximum values at a repetition rate of 8 kHz and at an applied voltage of 12 kV. Thus, the optimum repetition rate and the optimum applied voltage for the energy efficiency of NO reduction are lower than the corresponding for the NO reduction.

These results for the NO reduction and energy efficiency were replotted as a function of the discharge power in Fig. 9. The NO reduction and the energy efficiency are well correlated with the discharge power. This fact can be explained as follows. The discharge power increases in proportion to the repetition rate, and it increases linearly with increasing applied voltage at a constant repetition rate, as shown in Fig. 4. The former is due to a fixed value of energy input per one



(a)



(b)

FIG. 10.  $\text{NH}_3$ -concentration dependencies of (a) NO reduction and (b) its energy efficiency at applied voltages  $V_{pp}$  of 4, 8, and 12 kV.

pulse, and the latter is attributable to the increase in the number of discharge, because the voltage applicable to the gap during discharge is fixed in dielectric barrier discharge. In other words, the NO reduction is determined by the total discharge time, because the discharge power is proportional to the total discharge time for changes in both the applied voltage and the repetition rate. Figure 9(b) shows that the energy efficiency increases with decreasing the discharge power and that the maximum value is obtained near the lowest discharge power. This fact has been reported also for the  $\text{NO}_x$  removal via oxidation process,<sup>4-8</sup> and it is generally known that the energy efficiency in plasma chemical process, such as the conventional NO reduction system, ozonizer, etc., decreases with increasing the power.<sup>5</sup> Therefore, the ammonia radicals should be produced by the electron-impact dissociation of  $\text{NH}_3$ , which is the most energetically efficient way for producing the radicals.

Figure 10 shows the NO reduction and its energy efficiency at applied voltages  $V_{pp}$  of 4, 8, and 12 kV as a function of  $\text{NH}_3$  concentration. At each applied voltage, the NO reduction and the energy efficiency depend strongly on  $\text{NH}_3$  concentration, showing the maximum values at the same value of  $\text{NH}_3$  concentration. The  $\text{NH}_3$  concentration windows of effective NO reduction is narrow, suggesting that the fraction of the ammonia radicals ( $\text{NH}_2$ ,  $\text{NH}$ , and  $\text{N}$ ), which are produced by electron-impact dissociation of  $\text{NH}_3$ , de-

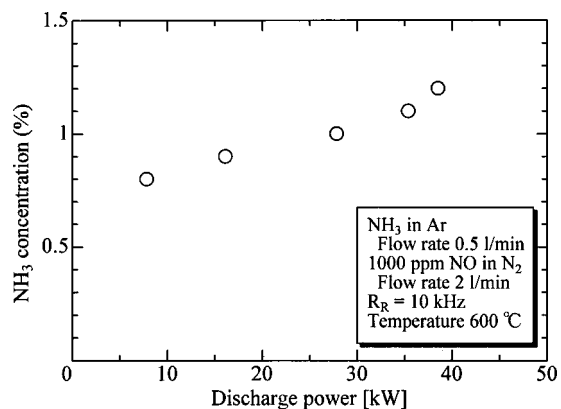


FIG. 11. Optimum  $\text{NH}_3$  concentration for energy efficiency of NO reduction as a function of discharge power.

depends on the concentration of  $\text{NH}_3$ , and that the fraction of the primary reducing agent,  $\text{NH}_2$  radical, is larger at the effective  $\text{NH}_3$  concentration. The maximum value of NO reduction at each optimum  $\text{NH}_3$  concentration decreases but the maximum value of energy efficiency increases with decreasing applied voltage, indicating that a lower applied voltage shows the maximum energy efficiency in a way similar to that for a constant  $\text{NH}_3$  concentration as shown in Fig. 9(b). Figure 11 shows the optimum  $\text{NH}_3$  concentration for the energy efficiency of NO reduction as a function of discharge power. The optimum  $\text{NH}_3$  concentration weakly depends on discharge power, and decreases with decreasing discharge power, indicating that a lower  $\text{NH}_3$  concentration is optimum for a lower discharge power.

The highest energy efficiency, 24 g/kWh, was obtained at a  $\text{NH}_3$  concentration of 0.3%, at an applied voltage of 5 kV, and at a repetition rate of 2.5 kHz. The corresponding specific energy consumption is 46.6 eV per NO molecule. Penetrante *et al.*<sup>11</sup> reported the specific energy consumption of 240 eV per NO molecule; the larger value is attributable to the larger dissociation energy of  $\text{N}_2$  compared to that of

$\text{NH}_3$ . A similar value of the energy efficiency, 20 g/kWh, has been reported for the NO removal via oxidation process in NO-air mixture using corona discharge,<sup>4</sup> although the dissociation energy of  $\text{O}_2$  is low compared to those of  $\text{NH}_3$ .

#### IV. CONCLUSIONS

NO in  $\text{N}_2$  gas can be removed by injecting ammonia radicals, which were externally generated by flowing the  $\text{NH}_3$  gas diluted with Ar gas through dielectric barrier discharge with a one-cycle sinusoidal-wave power source. The NO reductions for changes in both the applied voltage and the repetition rate are well correlated with the discharge power, which is proportional to the total discharge time per unit time. There is an optimum  $\text{NH}_3$  concentration in the narrow concentration window for the energy efficiency of NO reduction at a fixed discharge power. The maximum energy efficiency is obtained at small values of the  $\text{NH}_3$  concentration and the discharge power. The low  $\text{NH}_3$  concentration effectively increases the energy efficiency by drastically decreasing the discharge-firing voltage.

- <sup>1</sup>R. K. Lyon, *Int. J. Chem. Kinet.* **8**, 315 (1976).
- <sup>2</sup>J. A. Miller, M. C. Branch, and R. J. Kee, *Combust. Flame* **43**, 81 (1981).
- <sup>3</sup>J. A. Miller and C. T. Bowman, *Prog. Energy Combust. Sci.* **15**, 287 (1989).
- <sup>4</sup>S. Masuda and H. Nakao, *IEEE Trans. Ind. Appl.* **26**, 374 (1990).
- <sup>5</sup>T. Ohkubo, S. Kanazawa, Y. Nomoto, J. S. Chang, and T. Adachi, *IEEE Trans. Ind. Appl.* **30**, 856 (1994).
- <sup>6</sup>J. S. Chang, P. C. Looy, K. Nagai, T. Yoshioka, S. Aoki, and A. Maezawa, *IEEE Trans. Ind. Appl.* **32**, 131 (1996).
- <sup>7</sup>S. Kanazawa, J. S. Chang, G. F. Round, G. Sheng, T. Ohkubo, Y. Nomoto, and T. Adachi, *Combust. Sci. Technol.* **133**, 93 (1998).
- <sup>8</sup>R. Dorai and M. J. Kushner, *J. Appl. Phys.* **88**, 3739 (2000).
- <sup>9</sup>Q. Zhou, S.-C. Yao, A. Russell, and J. Boyle, *J. Air Waste Manag. Assoc.* **42**, 1193 (1992).
- <sup>10</sup>J. Boyle, A. Russell, S.-C. Yao, Q. Zhou, J. Ekmann, Y. Fu, and M. Mathur, *Fuel* **72**, 1419 (1993).
- <sup>11</sup>B. M. Penetrante, M. C. Hsiao, B. T. Merritt, G. E. Vogtlin, and P. H. Wallman, *IEEE Trans. Plasma Sci.* **23**, 679 (1995).
- <sup>12</sup>S. Hashimoto, *J. IEE Jpn.* **119**, 278 (1999) (in Japanese).
- <sup>13</sup>J. S. Chang, *Oyo Butsuri* **69**, 268 (2000) (in Japanese).